

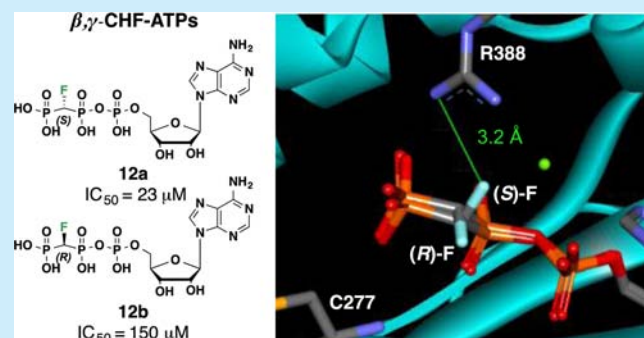
## 5'- $\beta,\gamma$ -CHF-ATP Diastereomers: Synthesis and Fluorine-Mediated Selective Binding by c-Src Protein Kinase

Candy S. Hwang,<sup>†</sup> Alvin Kung,<sup>†,‡</sup> Boris A. Kashemirov,<sup>†</sup> Chao Zhang,<sup>†,‡</sup> and Charles E. McKenna<sup>\*,†</sup>

<sup>†</sup>Department of Chemistry and <sup>‡</sup>Loker Hydrocarbon Research Institute, University of Southern California, Los Angeles, California 90089, United States

**S** Supporting Information

**ABSTRACT:** The first preparation of the individual  $\beta,\gamma$ -CHF-ATP stereoisomers **12a** and **12b** is reported. Configurationally differing solely by the orientation of the C–F fluorine, **12a** and **12b** have discrete <sup>31</sup>P (202 MHz, pH 10.9,  $\Delta\delta_{p\alpha}$  6 Hz,  $\Delta\delta_{p\beta}$  4 Hz) and <sup>19</sup>F NMR (470 MHz, pH 9.8,  $\Delta\delta_F$  25 Hz) spectral signatures and exhibit a 6-fold difference in IC<sub>50</sub> values for c-Src kinase, attributed to a unique interaction of the (S)-fluorine of bound **12b** with R388 in the active site.



ATP is ubiquitous in biological systems where it plays a central role in energy storage, transduction, and utilization. Modification of the triphosphate moiety by replacing the oxygen between the  $\beta$ - and  $\gamma$ -phosphate with a methylene ( $\text{CH}_2$ )<sup>1</sup> creates nonhydrolyzable inhibitors for enzymes that cleave the  $\gamma$ -phosphate, such as ATPases and protein kinases.<sup>2,3</sup> It was proposed many years ago that  $\alpha$ -fluorination of the bridging methylene affords pCHFp analogues (CXY, X, Y = HF) that are more isoacidic with ATP than the corresponding pCH<sub>2</sub>p analogues.<sup>4–6</sup> Besides adjusting the electronegativity of the bridging carbon to more closely resemble that of the bridging oxygen atom with minimal steric perturbation, the general absence of the fluorine atom from natural biological systems allows it to function as a bioorthogonal and readily detectable probe for <sup>19</sup>F NMR studies. At the same time, replacement of the pOp oxygen by CHF introduces a new chiral center into the nucleotide, resulting in two diastereomeric forms of  $\beta,\gamma$ -CHF-ATP that offer the potential advantage of comparing biochemical properties of two enzyme inhibitors essentially identical in structure except with respect to the orientation of the C–F fluorine within a protein binding site. By switching a defined fluorine orientation in an otherwise similarly bound ATP analogue, a unique platform for investigating weak F bonding interactions<sup>7–11</sup> with proteins is thus made available.

Beginning in the late 1990s, reports began to appear<sup>12–15</sup> suggesting that the CHF stereochemistry of  $\alpha$ -fluorinated monophosphonates can affect their binding to enzymes, and interest in this phenomenon has continued to grow.<sup>9,16–18</sup> However, the preparation of the individual diastereomers of  $\beta,\gamma$ -CHF-ATP itself has remained an unmet challenge, preventing this unique set of enzyme probes from realizing their original potential. Standard approaches to the synthesis of

$\beta,\gamma$ -CXY ATPs such as conjugation of the appropriate methylenebis(phosphonic acid) salt with a 5'-activated AMP<sup>19</sup> (Figure 1) result in a mixture of both diastereomers when X  $\neq$  Y.

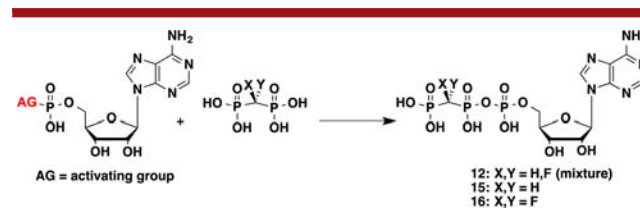


**Figure 1.** Standard synthesis of  $\beta,\gamma$ -CXY-ATPs.

$\beta,\gamma$ -CXY and  $\alpha,\beta$ -CXY desoxyNTP analogues have recently demonstrated their utility as probes of the ground and transition states of DNA polymerase  $\beta$  (pol  $\beta$ ).<sup>20–24</sup> As part of these studies, the individual synthesis of all four  $\beta,\gamma$ -CHF and  $\beta,\gamma$ -CHCl dGTP diastereomers was achieved, with the absolute configurations assigned by X-ray crystallography of their ternary complex with DNA and pol  $\beta$ .<sup>25</sup> These analogues were found to exhibit significantly different  $K_d$  and  $k_{pol}$  values with the enzyme, modulated only by the position of the halogen atom substituent at the CXY carbon.<sup>24</sup> Furthermore, the <sup>19</sup>F NMR spectra of these CHF diastereomers were found to be resolvable and useful to monitor their stereoselective turnover catalyzed by the enzyme.<sup>20,24</sup> Early work on synthetic  $\beta,\gamma$ -CHF-ATP mixtures<sup>26</sup> and a recent paper on  $\beta,\gamma$ -CHF-UTPs<sup>18</sup> reported inability to distinguish the ribosynucleotide CHF-

**Received:** December 31, 2014

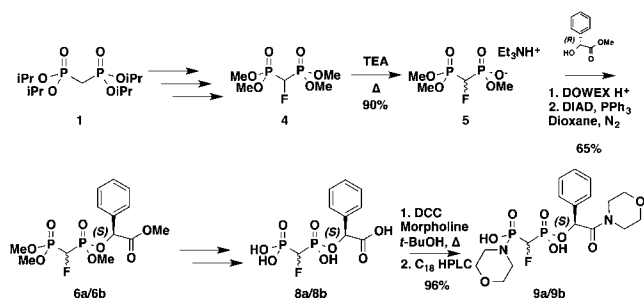
**Revised:** February 28, 2015

**Published:** March 17, 2015

stereoisomers by  $^{19}\text{F}$  NMR, although the former observation was not confirmed when the fluorinated ATP derivative was prepared by an alternate method.<sup>27</sup>

These results prompted us to attempt the long-awaited synthesis of the individual  $\beta,\gamma$ -CHF-ATPs. Our strategy was based on the key chiral bisphosphonate synthons **9a** and **9b** (separable by preparative HPLC) prepared in eight steps from tetraisopropyl methylenebis(phosphonate) **1**;<sup>25</sup> however, the synthesis of **9a** and **9b** was modified at several steps, improving the yield significantly (Scheme 1). In the first modification,

### Scheme 1. Modified Synthesis of (S)-Mandelic Acid Morpholinamide (R)/(S)-Monoesters **9a** and **9b**



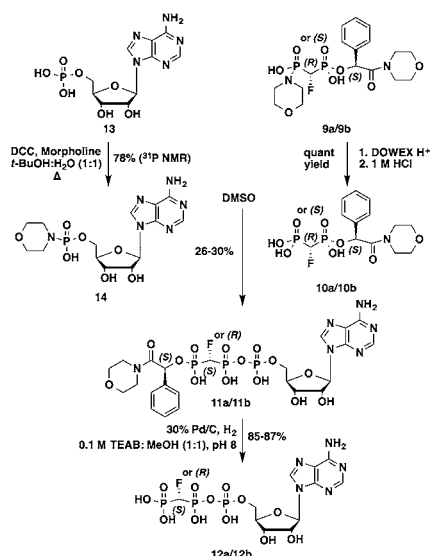
monodemethylation of **4** (previously prepared with NaI<sup>25</sup>) with triethylamine<sup>28,29</sup> under reflux raised the isolated yield of **5** to 90% with a substantial reduction in reaction time to 10–20 min.

Compound **5** was then transformed into the stereoisomer ester mixture **6a/6b**, purified on a silica gel column replacing the original preparative TLC procedure for convenient scalability.<sup>25</sup> In the second important modification, after conversion of **6a/6b** to the acids **8a/8b**,<sup>25</sup> the latter were derivatized to the chiral dimorpholidates **9a/9b** using a nonaqueous solvent system, shortening the reaction time from several hours to <1 h after addition of DCC and also modestly increasing the yield from 87% to 96%, additionally aided by a more performant reversed-phase HPLC column.

Prior to separation and purification of the individual isomers, reaction mixture **9a/9b** taken up in D<sub>2</sub>O showed discrete, but overlapping, multiplets in the  $^{19}\text{F}$  (470 or 564 MHz, pH 8.8–9.3, Figures S7C,D and S11, Supporting Information) and  $^{31}\text{P}$  NMR spectra (202 MHz, pH 8.8–8.9, Figures S9 and S13, Supporting Information). Interestingly, the same sample dissolved in CD<sub>3</sub>OD gave a clean separation between the isomer multiplets in  $^{19}\text{F}$  NMR (470 or 564 MHz, Figures S7A,B and S10, Supporting Information), but the relative position of the two resonances was inverted, which was confirmed at higher spectrometer frequency (564 MHz) and by spiking with **9a** (Figure S10–11, Supporting Information).

The separated individual isomers in acid form (**10a**, **10b**)<sup>25</sup> were coupled conventionally with AMP-morpholidate<sup>19</sup> (AMP 5'-M, **14**) and then treated to remove the protecting groups as described previously<sup>25</sup> (Scheme 2). Gratifyingly, coupling of **14** to the individual synthons did not require additional protection of the 2',3'-hydroxyl groups of the ribose sugar. The (R)/(S)-CHF chirality of the separated and purified dimorpholidated chiral synthons (**9a** and **9b**) was assigned by HPLC and NMR analysis in comparison with the literature values.<sup>25</sup>  $^{31}\text{P}$  NMR spectral splitting patterns in D<sub>2</sub>O (Figures S20 and S24, Supporting Information), where **9a** exhibits second order splitting, additionally distinguish the two isomers. (The original

### Scheme 2. Synthesis of **12a** and **12b** from **9a** and **9b**, Respectively



assignments of the absolute configurations of **9a** and **9b** were established retrosynthetically from the X-ray structure of (R)- $\beta,\gamma$ -CHF-dGTP complexed to DNA pol.<sup>25</sup>)

$\beta,\gamma$ -Methylene (CH<sub>2</sub>)-, mixed  $\beta,\gamma$ -CHF-, and  $\beta,\gamma$ -difluoromethylene (CF<sub>2</sub>)-ATPs were synthesized by conjugating **14** with the appropriate bisphosphonate (Figure 1).<sup>1,6,19</sup> A discrete  $^{19}\text{F}$  and  $^{31}\text{P}$  NMR spectrum for each diastereomer **12a/12b** in a synthetic mixture (**12**) was observed (Figures S44 and S45, Supporting Information), contrary to early observations<sup>26</sup> but consistent with prior observations for  $\beta,\gamma$ -CHF-dGTP<sup>20,22,25</sup> and -UTP analogues.<sup>30</sup> The discrepancy may be attributed to the crucial role of the sample pH<sup>31</sup> ( $\geq 10$ ) and, possibly, the nature of the counteranion (e.g., NH<sub>4</sub><sup>+</sup> gives broadened line widths).<sup>30,32</sup> A 3:1 mixture of the separated diastereomers was made, and its  $^{19}\text{F}$  and  $^{31}\text{P}$  NMR spectra were measured to confirm (Figures S55 and S56, Supporting Information) that **12a** (the (S)-CHF-isomer) resonates more downfield in the  $^{19}\text{F}$  NMR and has P <sub>$\alpha$</sub>  and P <sub>$\beta$</sub>  more downfield and upfield, respectively, in the  $^{31}\text{P}$  NMR.<sup>25</sup> To further validate the assignment of each pairwise resonance<sup>25</sup> to a specific diastereomer, the  $^{19}\text{F}$  NMR spectra were simulated<sup>33</sup> and compared to that of the experimental mixture of isomers (Figure S57, Supporting Information).<sup>22,30</sup> The ability to discern each diastereomer by  $^{19}\text{F}$  and  $^{31}\text{P}$  NMR provides a convenient method for determining selective substrate consumption by a selective enzyme.<sup>18,24</sup>

In search of an enzyme interaction that might be stereospecific for **12a** vs **12b**, we examined a protein kinase. Protein kinases catalyze the transfer of a phosphoryl group from ATP to substrate proteins. As a major mode of post-translational modification, the phosphorylation event catalyzed by protein kinases regulates fundamental cellular processes such as cell proliferation, differentiation and motility. Aberrant expression or activation of these enzymes can often lead to a variety of human diseases.<sup>34–38</sup> For example, overexpression of Src tyrosine kinases is frequently found in cancerous tumors.<sup>3,34,39–41</sup> Understanding the catalytic mechanism of Src and its role in oncogenesis is critical for design of therapeutic agents to target the diseases associated with its dysregulation.<sup>3,37–40</sup>

We tested the  $\beta,\gamma$ -CXY-ATP analogues **12**, **15**, and **16**, (Figure 1) as inhibitors against the kinase domain of Src (c-Src, E.C. 2.7.10.2) and determined their  $IC_{50}$  values using the radioactive disk assay.<sup>42</sup> The data from the inhibition assays show that fluorination at the  $\beta,\gamma$ -position increases inhibitor potency (Table 1).  $\beta,\gamma$ -CH<sub>2</sub>-ATP (**15**) was already shown to be

**Table 1. Effect of Fluorination of  $\beta,\gamma$ -CH<sub>2</sub>-ATP on Inhibition of c-Src Kinase**

$IC_{50}$	X, Y = H <sub>2</sub> <b>15</b> ( $\mu$ M)	X, Y = HF <b>12</b> ( $\mu$ M)	X, Y = F <sub>2</sub> <b>16</b> ( $\mu$ M)
mean $\pm$ SE ( <i>n</i> ) <sup>a</sup>	145 $\pm$ 25 (3)	47 $\pm$ 7 (6)	46 $\pm$ 7 (3)

<sup>a</sup>SE = standard error; *n* = number of replicates; variance test revealed no significant deviation prior to running an ANOVA. Differences (ANOVA, *F* (2, 6) = 12, *p* = 0.008 < 0.05) are statistically significant.

a competitive inhibitor of c-Src kinase with respect to ATP and a noncompetitive inhibitor versus the peptide substrate.<sup>2</sup> The  $K_m$  for ATP and c-Src kinase is reported at around 80  $\mu$ M.<sup>43</sup>

The Src kinase inhibition assay  $IC_{50}$  data (Table 2) indicate a 6-fold selectivity for the (*S*)-CHF-ATP diastereomer **12a**. The

**Table 2. Inhibition of c-Src Kinase by  $\beta,\gamma$ -CHF-ATP Diastereomers**

$IC_{50}$	X, Y = H, F <b>12a</b> ( $\mu$ M)	X, Y = F, H <b>12b</b> ( $\mu$ M)	mixture (~1:1) <b>12</b> ( $\mu$ M)
mean $\pm$ SE ( <i>n</i> ) <sup>a</sup>	23 $\pm$ 4 (6)	150 $\pm$ 8 (5)	47 $\pm$ 7 (6)

<sup>a</sup>SE = standard error; *n* = number of replicates; variance test revealed no significant deviation prior to ANOVA. Differences (ANOVA, *F* (2, 12) = 105, *p* < 0.001) are statistically significant.

relative potency of **16** appears to exclude a steric origin for the selectivity exhibited by the enzyme. We hypothesize that the specific orientation of the CHF-fluorine in **12a** makes possible a specific dipolar interaction, adding additional stabilization energy to the complex, which is reflected in the  $IC_{50}$  difference. To examine this possibility, in silico molecular docking simulations using AutoDock Vina 1.1.2<sup>44</sup> were performed to explore potential protein–ligand interactions (Figure 2). Although our kinase assays were performed using chicken Src kinase, we chose a published X-ray crystal structure of human Src (2SRC) for molecular docking calculations due to the higher resolution available (1.8 Å vs 2.3 Å for chicken Src

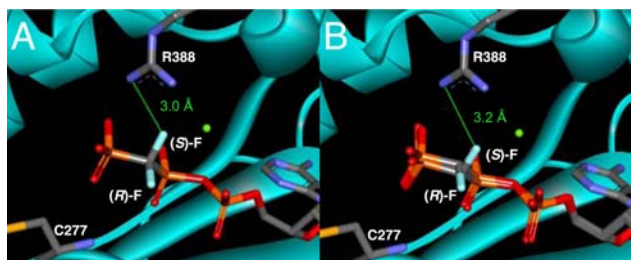


**Figure 2.** Superimposition for (A) **16** and (B) **12a** and **12b** docked into the active site of human Src kinase using AutoDock Vina 1.1.2 and X-ray crystallographic data for the apoprotein (2SRC) including Mg (shown as green sphere). The (*S*)-fluorine in both compounds is oriented toward Arg388. The (*R*)-fluorine is oriented toward the pocket entrance, with no protein atoms closer than 3.8 Å. The figures were generated using Accelerlys Discovery Studio.<sup>53</sup>

(3DQX)). The human and chicken Src proteins share 99% sequence identity (using BLASTP 2.2.30+<sup>45</sup>) and are identical within the active site.<sup>46</sup>

The calculations suggested interactions of both the (*S*)-fluorine of **16** and the  $\gamma$ -phosphate with the active site Arg388 (the latter observation is consistent with the crystal structure of c-Src kinase<sup>47</sup>): the (*S*)-fluorine atom of **16** is located 3.0 Å from a guanidinium N of Arg388 (Figure 2A). Additionally, Lys295 stabilizes two phosphates, and Asp404 interacts with a structural water and Mg<sup>2+</sup>. In contrast, interactions of the (*R*)-fluorine with residues in the active site were not identified: the nearest group was the amido NH of Cys277 at 3.6 Å, too distant from the (*R*)-fluorine to have a significant interaction (Figure 2A). The (*R*)-fluorine was found to be 3.8 Å from the carbonyl carbon of Gly276 and 4.6 Å from the nearer N of Arg388.

Fluorine atoms proximal to Arg side chain nitrogens have been frequently documented in the literature,<sup>14,48</sup> and it has been proposed that the guanidinium moiety of Arg is fluorophilic.<sup>49–51</sup> We previously observed an apparent interaction of the CHF-fluorine of  $\beta,\gamma$ -CHF-dGTP with Arg183 (PDB entry 4DO9) in the nucleotide-binding site of pol  $\beta$ .<sup>20,22,25</sup> The  $IC_{50}$  ratio of 6:1 observed for **12b** vs **12a** corresponds to a bonding interaction on the order of 1.1 kcal/mol, which is consistent with literature values for weak noncovalent fluorine bonds.<sup>49,52</sup>

In summary, for the first time, the individual diastereomers of  $\beta,\gamma$ -CHF-ATP have been obtained using an improved method for preparing the separable (*S*)-mandelic acid morpholinamide (*R*)/(*S*)-monoesters **9a** and **9b** as synthons. The two diastereomers have discrete <sup>19</sup>F and <sup>31</sup>P NMR spectra in D<sub>2</sub>O and CD<sub>3</sub>OD and show significantly different inhibition constants for c-Src protein kinase, associated with the presence or absence of a noncovalent bonding interaction of C–F with R388 in the active site.

## ■ ASSOCIATED CONTENT

### § Supporting Information

Detailed information on the synthesis of **4–12** and **14–17** including, <sup>1</sup>H, <sup>19</sup>F, and <sup>31</sup>P NMR and MS spectra and HPLC analytical and preparative traces. Experimental conditions and data for enzyme and characterization assays. Details of molecular docking studies. This material is available free of charge via the Internet at <http://pubs.acs.org>.

## ■ AUTHOR INFORMATION

### Corresponding Author

\*E-mail: [mckenna@usc.edu](mailto:mckenna@usc.edu).

### Notes

The authors declare no competing financial interest.

## ■ ACKNOWLEDGMENTS

This work was supported by funding from the Dana and David Dornsife College of the University of Southern California (C.E.M. and C.Z.) and NIH U19CA177547 (C.E.M.) and by a National Science Foundation Graduate Research Fellowship (to C.S.H., DGE-0937362).

## ■ REFERENCES

- (1) Myers, T. C.; Nakamura, K.; Flesher, J. W. *J. Am. Chem. Soc.* **1963**, *85*, 3292.

- (2) Boerner, R. J.; Barker, S. C.; Knight, W. B. *Biochemistry* **1995**, *34*, 16419.
- (3) Elphick, L. M.; Lee, S. E.; Gouverneur, V.; Mann, D. J. *ACS Chem. Biol.* **2007**, *2*, 299.
- (4) McKenna, C. E.; Shen, P. D. *J. Org. Chem.* **1981**, *46*, 4573.
- (5) Leswara, N. D.; Shen, P. D.; McKenna, C. E. *Fed. Proc.* **1982**, *41*, 860.
- (6) Blackburn, G. M.; Kent, D. E.; Kolkman, F. J. *Chem. Soc., Chem. Commun.* **1981**, 1188.
- (7) Dalvit, C.; Vulpetti, A. *ChemMedChem* **2011**, *6*, 104.
- (8) O'Hagan, D. *Chem. Soc. Rev.* **2008**, *37*, 308.
- (9) Berkowitz, D. B.; Karukurichi, K. R.; de la Salud-Bea, R.; Nelson, D. L.; McCune, C. D. *J. Fluorine Chem.* **2008**, *129*, 731.
- (10) Romanenko, V. D.; Kukhar, V. P. *Chem. Rev.* **2006**, *106*, 3868–3935.
- (11) Bégué, J.-P.; Bonnet-Delpon, D. *J. Fluorine Chem.* **2006**, *127*, 992.
- (12) Nieschalk, J.; Batsanov, A. S.; O'Hagan, D.; Howard, J. *Tetrahedron* **1996**, *52*, 165.
- (13) Berkowitz, D. B.; Bose, M.; Pfannenstiel, T. J.; Doukov, T. J. *Org. Chem.* **2000**, *65*, 4498.
- (14) Berkowitz, D. B.; Bose, M. *J. Fluorine Chem.* **2001**, *112*, 13.
- (15) Xu, Y.; Qian, L.; Prestwich, G. D. *J. Org. Chem.* **2003**, *68*, 5320.
- (16) Cox, R. J.; Gibson, J. S.; Hadfield, A. T. *ChemBioChem* **2005**, *6*, 2255.
- (17) Forget, S. M.; Bhattasali, D.; Hart, V. C.; Cameron, T. S.; Syvitski, R. T.; Jakeman, D. L. *Chem. Sci.* **2012**, *3*, 1866.
- (18) Beaton, S. A.; Jiang, P. M.; Melong, J. C.; Loranger, M. W.; Mohamady, S.; Veinot, T. I.; Jakeman, D. L. *Org. Biomol. Chem.* **2013**, *11*, 5473.
- (19) Roseman, S.; Distler, J. J.; Moffatt, J. G.; Khorana, H. G. *J. Am. Chem. Soc.* **1961**, *83*, 659.
- (20) McKenna, C. E.; Kashemirov, B. A.; Upton, T. G.; Batra, V. K.; Goodman, M. F.; Pedersen, L. C.; Beard, W. A.; Wilson, S. H. *J. Am. Chem. Soc.* **2007**, *129*, 15412.
- (21) Sucato, C. A.; Upton, T. G.; Kashemirov, B. A.; Batra, V. K.; Martinek, V.; Xiang, Y.; Beard, W. A.; Pedersen, L. C.; Wilson, S. H.; McKenna, C. E.; Florian, J.; Warshel, A.; Goodman, M. F. *Biochemistry* **2007**, *46*, 461.
- (22) Batra, V. K.; Pedersen, L. C.; Beard, W. A.; Wilson, S. H.; Kashemirov, B. A.; Upton, T. G.; Goodman, M. F.; McKenna, C. E. *J. Am. Chem. Soc.* **2010**, *132*, 7617.
- (23) Sucato, C. A.; Upton, T. G.; Kashemirov, B. A.; Osuna, J.; Oertell, K.; Beard, W. A.; Wilson, S. H.; Florian, J.; Warshel, A.; McKenna, C. E.; Goodman, M. F. *Biochemistry* **2008**, *47*, 870.
- (24) Oertell, K.; Wu, Y.; Zakharova, V. M.; Kashemirov, B. A.; Shock, D. D.; Beard, W. A.; Wilson, S. H.; McKenna, C. E.; Goodman, M. F. *Biochemistry* **2012**, *51*, 8491.
- (25) Wu, Y.; Zakharova, V. M.; Kashemirov, B. A.; Goodman, M. F.; Batra, V. K.; Wilson, S. H.; McKenna, C. E. *J. Am. Chem. Soc.* **2012**, *134*, 8734.
- (26) Blackburn, G. M.; Kent, D. E.; Kolkman, F. J. *Chem. Soc., Perkin Trans. 1* **1984**, 1119.
- (27) McKenna, C. E.; Harutunian, V. *FASEB J.* **1988**, *2*, 6148.
- (28) Vepsäläinen, J. J.; Kivikoski, J.; Ahlgrén, M.; Nupponen, H. E.; Pohjala, E. K. *Tetrahedron* **1995**, *51*, 6805.
- (29) Ahlmark, M. J.; Vepsäläinen, J. J. *Tetrahedron* **1997**, *53*, 16153.
- (30) Hwang, C. S.; Kashemirov, B. A.; McKenna, C. E. *J. Org. Chem.* **2014**, *79*, 5315.
- (31) The pH values for deuterated water solutions as reported here and by us previously (refs 20, 22, 25, 30) are given as measured with a glass electrode, without correction to pD (ref 32).
- (32) Krężel, A.; Bal, W. *J. Inorg. Biochem.* **2004**, *98*, 161.
- (33) Fluorine NMR were simulated using spin simulation on MestReNova 8.1.2.
- (34) Schwartz, P. A.; Murray, B. W. *Bioorg. Chem.* **2011**, *39*, 192.
- (35) Kalesh, K. A.; Liu, K.; Yao, S. Q. *Org. Biomol. Chem.* **2009**, *7*, 5129.
- (36) Xie, J.; Corneau, A. B.; Seto, C. T. *Org. Lett.* **2003**, *6*, 83.
- (37) Moffat, D.; Nichols, C. J.; Riley, D. A.; Simpkins, N. S. *Org. Biomol. Chem.* **2005**, *3*, 2953.
- (38) Zhang, C.; Lopez, M. S.; Dar, A. C.; Ladow, E.; Finkbeiner, S.; Yun, C. H.; Eck, M. J.; Shokat, K. M. *ACS Chem. Biol.* **2013**, *8*, 1931.
- (39) Kwarczynski, F. E.; Fox, C. C.; Steffey, M. E.; Soellner, M. B. *ACS Chem. Biol.* **2012**, *7*, 1910.
- (40) Brandvold, K. R.; Steffey, M. E.; Fox, C. C.; Soellner, M. B. *ACS Chem. Biol.* **2012**, *7*, 1393.
- (41) Ulrich, S. M.; Kenski, D. M.; Shokat, K. M. *Biochemistry* **2003**, *42*, 7915.
- (42) Witt, J. J.; Roskoski, R., Jr. *Anal. Biochem.* **1975**, *66*, 253.
- (43) Knight, Z. A.; Shokat, K. M. *Chem. Biol.* **2005**, *12*, 621.
- (44) Trott, O.; Olson, A. J. *J. Comput. Chem.* **2010**, *31*, 455.
- (45) Altschul, S. F.; Madden, T. L.; Schäffer, A. A.; Zhang, J.; Zhang, Z.; Miller, W.; Lipman, D. J. *Nucleic Acids Res.* **1997**, *25*, 3389.
- (46) Via visual inspection of the active site using PyMol, The PyMOL Molecular Graphics System, Version 1.2r3pre, Schrödinger, LLC.
- (47) Xu, W.; Harrison, S. C.; Eck, M. J. *Nature* **1997**, *385*, 595.
- (48) Morgenthaler, M.; Aebi, J. D.; Grüniger, F.; Mona, D.; Wagner, B.; Kansy, M.; Diederich, F. *J. Fluorine Chem.* **2008**, *129*, 852.
- (49) Zhou, P.; Zou, J.; Tian, F.; Shang, Z. *J. Chem. Inf. Model.* **2009**, *49*, 2344.
- (50) Muller, K.; Faeh, C.; Diederich, F. *Science* **2007**, *317*, 1881.
- (51) Hagmann, W. K. *J. Med. Chem.* **2008**, *51*, 4359.
- (52) Dalvit, C.; Invernizzi, C.; Vulpetti, A. *Chem.—Eur. J.* **2014**, *20*, 11058.
- (53) Accelrys Software, Inc. *Discovery Studio Modeling Environment*, Release 4.1; Accelrys Software, Inc., San Diego, 2007.